Available online at www.sciencedirect.com
ScienceDirect
Journal of the European Ceramic Society 30 (2010) 503–508
www.elsevier.com/locate/jeurceramsoc

Electrical properties of Li-doped NiO films

Wei-Luen Jang [a], Yang-Ming Lu [b], Weng-Sing Hwang [a,*], Wei-Chien Chen [a]

[a] *Department of Materials Science and Engineering, National Cheng Kung University, No. 1, University Road, Tainan City 701, Taiwan, ROC*
[b] *Graduate Institute of Electro-Optics, National University of Tainan, No. 33, Sec. 2, Shu-Lin St., Tainan 700, Taiwan, ROC*

Available online 25 June 2009

Abstract

Lithium-doped NiO films were deposited by radio frequency magnetron sputtering on Corning 1737 glass substrates. The Li concentrations in the films varied from 0 to 16.29 at.%, as determined by wavelength-dispersive X-ray analysis and inductively coupled plasma mass spectrometry. The effects of Li content on properties such as microstructure, resistivity, and electrical stability were studied. The results show that the doped Li ions tend to occupy crystal defect sites such as vacancies or segregate on the film surface. Initially, doped Li occupied the nickel vacancies in the film, decreasing the electrical conductivity. When the Li concentration was further increased, some Li segregated on the film surface and formed bulges at high Li concentrations. These Li-rich oxides covering the film surface served as partitions between the film and moisture from the atmosphere. As a result, the Li-doped NiO films show a relatively high arrestment to electrical resistance aging.

Keywords: NiO; Li-doped; Electrical stability; Electrical properties

1. Introduction

NiO is a promising candidate for p-type semi-transparent conducting films with band gap energy from 3.6 to 4.0 eV.[1] Hence NiO film is transparent in visible light. Defect in NiO film formed Ni^{3+} ions which make the film black. The transmittance of the as-deposited NiO film is about 40% in the visible range, it can be as high as 80% after heat-treated at 300 °C.[1] NiO films have a wide range of applications, such as the anode material in organic light emitting diodes (OLED),[2] electrochromic display devices,[3] and gas sensors.[4] Although stoichiometric NiO is an insulator with a resistivity of 10^{13} Ω cm at room temperature, its resistivity can be lowered by an increase of Ni^{3+} ions, which results from the creation of nickel vacancies or by the incorporation of monovalent atoms such as Li in NiO crystallities.[5]

According to the literature, NiO films have been prepared by sputtering,[1] chemical vapor deposition,[6] and the spray pyrolysis process.[7] Among these methods, sputtering is the most widely used. Due to the non-equilibrium nature of sputtering, the defect concentration is higher than that for films prepared by other methods. The resistivity of sputtered NiO film can be as low as 1.4×10^{-1} Ω cm.[1] Li doping can also be used to increase the electrical conductivity of NiO films. Li-doped NiO films have been prepared using the spray pyrolysis technique[8] and the combinatorial pulse laser deposition technique.[9] However, the resistivity of Li-doped NiO films prepared by the above methods is ∼1 Ω cm, which is almost one order of magnitude higher than that of un-doped NiO films prepared by the sputtering process.

Hence, if Ni^{3+} ions contributed from nickel vacancies created by the sputtering process and the incorporation of Li atoms can coexist in the NiO films, the conductivity is expected to increase further. Stabilizing the electrical properties[10,11] is another important issue for applications of NiO films. Therefore, the effects of Li doping on the electrical stability of sputtered NiO films are also investigated.

2. Experimental methods

NiO films were deposited on Corning 1737 glass substrates by RF magnetron sputtering. The base pressure achieved was 6×10^{-3} Pa. Pure oxygen was used as the working gas (99.99%) during sputtering and the working pressure was kept at 1.33 Pa. The target material was ceramic NiO (99.99%). The target power was fixed at 200 W and the target area was about 26 cm^2. The concentrations of Li in the thin films were adjusted by placing 0–15 Li_2O disks on the target surface. The thickness and diameter of the Li_2O disks were controlled to be 0.2 and 1 cm, respectively. A rotating substrate holder was used to obtain a uniform composition of films.

* Corresponding author. Fax: +886 6 2344393.
E-mail address: wshwang@mail.ncku.edu.tw (W.-S. Hwang).

0955-2219/$ – see front matter © 2009 Elsevier Ltd. All rights reserved.
doi:10.1016/j.jeurceramsoc.2009.05.041

A conventional stylus surface-roughness detector (Alpha-step 200) was used to measure the film thickness. The thickness of the sputtered films was kept around 200 nm. The film composition was determined by a High Resolution Hyper Probe (JXA-8500F Fe-EPMA) equipped with a wavelength-dispersive X-ray spectrometer (WDS), an inductively coupled plasma mass spectrometer (Hewlett Packard 4500 ICP-MS), and an Auger electron nanoscope (ULVAC-PHI, PHI 700). The composition profiles were analyzed by a Secondary Ion Mass Spectrometer (Cameca IMS-4f SIMS) using a Cs^{1+} primary ion beam. For the SIMS measurement, a square area of 100 μm^2 was selected for analysis. The resistivity was measured by a four-probe system (Napson, RT-7). A field-emission scanning electron microscope (JSM-6700F) was used to examine the film microstructure. X-ray diffractometry measurements for film crystallography were carried out using a thin film diffractometer (Rigaku D/MAX2500) with monochromatic Cu Ka radiation.

In the electrical stability test, NiO film with a constant rectangular area of 1.5 cm^2 (1.0 cm × 1.5 cm) and a thickness of 200 nm was selected for a two-probe (probe distance of 0.5 cm) resistance test. The test was performed under humid Ar atmosphere at 20% RH (relative humidity at 25 °C) and the resistivity was recorded at every 10 min interval. As the two-probe measurements may be dominated by electrode contact effects, the film area, film thickness, test temperature, atmosphere and pressure were carefully controlled during the two-probe resistance test. In order to eliminate the electrode contact effects, the electrical stability of NiO films was determined by the change of resistance over time rather than the absolute value of resistance. It is believed that the electrode contact may have some effects on the resistance. However, the electrode contact resistance should not vary with time and the change of resistance should be a result of resistance change in the film itself. More details about stability test can be found in the literatures.[10,11]

3. Results and discussion

3.1. Composition of sputtered thin films

The properties of non-stoichiometric oxide semiconductors strongly depend on trace amounts of impurities and the atmosphere. Reaction parameters such as the substrate temperature, atmosphere, and fabrication techniques have a considerable effect on electrical properties. We thus fixed all other parameters and focused on studying the effect of dopant concentration on the electrical properties of NiO films.

The compositions of the doped NiO films were determined by WDS and ICP-MS. The O/Ni atomic ratios were obtained from WDS and the Li/Ni atomic ratios were measured by ICP-MS. Table 1 shows the Li–Ni–O ratios of the as-deposited films. The calculated Li atomic percentages and (Ni + Li/O) ratios are also listed in Table 1. Li concentration in the films increased with increasing number of Li_2O disks mounted on the NiO target surface. The maximum Li concentration obtained in this study was 16.29 at.%. The (Ni + Li/O) ratio increased and approached unity with increasing Li content which implies that the nickel vacancies decreased as Li was doped into the films.

Table 1
Li–Ni–O ratios of the sputtered NiO films.

Number of Li_2O	O	Ni	Li	(Ni + Li/O)	Calculated Li (at.%)
(a) 0	1.29	1	–	0.775	–
(b) 1	1.28	1	0.02	0.797	0.87
(c) 3	1.26	1	0.05	0.833	2.16
(d) 7	1.41	1	0.14	0.809	5.49
(e) 11	1.42	1	0.31	0.923	11.36
(f) 15	1.57	1	0.50	0.955	16.29

3.2. Effect of Li content on electrical resistivity

Fig. 1 shows film resistivity varying with Li concentration. Two stages of resistivity change were found as Li content increased in the NiO films. As shown in Fig. 1, the resistivity of un-doped NiO film was 2.08×10^{-1} Ω cm. This value increased with Li doping, reaching a maximum value of 4.53×10^{-1} Ω cm at a Li concentration of 2.16 at.%. The resistivity slightly decreased to 3.21×10^{-1} Ω cm when the Li concentration reached 16.29 at.%.

The change of Li concentration and nickel vacancies can be readily obtained as shown in Table 1. However, it is very difficult to know the ratio of holes to total cations since the nickel vacancy may be partially singly charged and partially doubly charged.[12,13] It is generally believed that charged nickel vacancies are the predominating point defects for electrical properties. The defect equilibria involving singly and doubly charged nickel vacancies are given by the following equations. If singly charged nickel vacancies dominate; $[V_{Ni}'] \gg [V_{Ni}'']$, then

$$p = [V_{Ni}'] = K_1^{1/2} p_{O_2}^{1/4} \quad (1)$$

If doubly charged nickel vacancies dominate; $[V_{Ni}''] \gg [V_{Ni}']$, then

$$\tfrac{1}{2} p = [V_{Ni}'] = \tfrac{1}{4} K_2^{1/3} p_{O_2}^{1/6} \quad (2)$$

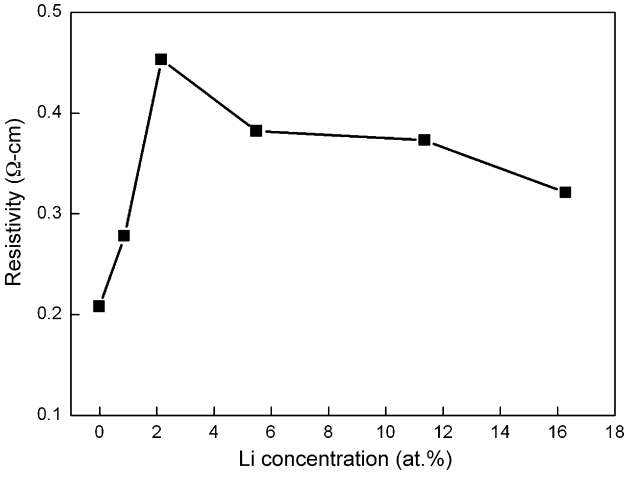

Fig. 1. Resistivity of NiO thin films with various Li concentrations.

where p denotes the concentration of electron holes (mole fraction of Ni^{3+} ions); [V_{Ni}'] and [V_{Ni}''] are the concentration of singly charged vacancy and doubly charged vacancy, respectively. p_{O_2} is the oxygen pressure (atm); K_1 and K_2 are reaction constants. It has been found in many investigations that the value of n in $p_{O_2}^{1/n}$ ranges from 4 to 6.[12,13] This suggests that the vacancies are partially singly and partially doubly charged. Since the relation between nickel vacancy and hole is not clear, the hole concentration cannot be simply obtained from the mass and charge balance.

Although the information of ratio of holes to total cations is not available, the relationship between composition and electrical properties can be explained through the change of nickel vacancy and Li concentration. According to Table 1, Li concentration increased and nickel vacancies decreased with increasing number of Li_2O disks. As a result, the hole contribution from nickel vacancies decreased. Conversely, the hole contribution from the incorporation of Li increased. Therefore, the effects of Li doping on electrical conductivity is due to a combination of decreased vacancies and increased Li concentration. The details of the reaction can be explained as follows.

Parravano and Boudart[5] assumed that the formation of a solid solution of NiO–Li_2O at small concentrations of Li oxide involves the filling of cationic vacancies in the lattice of NiO by Li ions. Considering double charged Ni vacancies, the formation of native cationic vacancies can be schematically described as Eq. (3), which is responsible for the electrical conduction of NiO film.

$$\frac{1}{2}O_2^{(g)} \leftrightarrow O_O^{\times} + V_{Ni}'' + 2\dot{h} \quad (3)$$

There is a large difference in the composition between sputtered and thermo-oxidized nickel oxide. When thermo-oxidized at 900 °C in 1 atm oxygen atmosphere, the y value in non-stoichiometric $Ni_{1-y}O$ is only approximately 10^{-4}.[13] In this study, the y value in $Ni_{1-y}O$ for the un-doped NiO film is about 0.22, which is considerably higher than the value found in thermo-oxidized nickel. This suggests that the as-sputtered NiO film contains many nickel vacancies. Doping with Li during the sputtering process makes nickel vacancies be occupied by Li, which can be represented by Eq. (4).

$$Li_2O + 2V_{Ni}'' + 2\dot{h} \leftrightarrow 2Li_{Ni}' + \frac{1}{2}O_2^{(g)} \quad (4)$$

Some electric holes are consumed at the same time to maintain electric neutrality. This increases the resistivity of the Li-doped NiO film, as shown in Fig. 1. From defect Eq. (4) and the composition change described in Section 3.2, initially the incorporated Li ions occupy the native Ni vacancies, consuming the electric hole concentration and lowing the non-stoichiometry of the NiO film. Therefore, the initial increase in resistivity and the decrease in excess oxygen content for samples (b) and (c) resulted from Li ions filling nickel vacancies during the sputtering process.

With increased Li doped into the film, some Li ions may substitute Ni^{2+} in the normal crystal sites and create new holes,

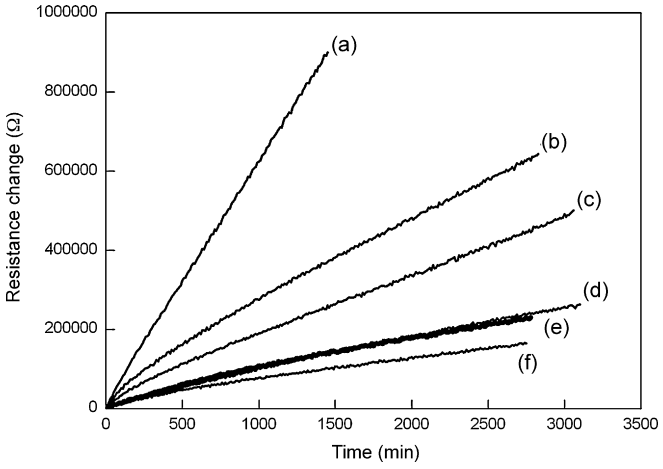

Fig. 2. Electrical aging behaviour of NiO films with various Li concentrations. (a) un-doped, (b) 0.87 at.% Li, (c) 2.16 at.% Li, (d) 5.49 at.% Li, (e) 11.36 at.% Li, and (f) 16.29 at.% Li.

as shown in Eq. (5). This leads to a slight decrease in resistivity.

$$\frac{1}{2}O_2^{(g)} + Li_2O \leftrightarrow 2O_O^{\times} + 2Li_{Ni}' + 2\dot{h} \quad (5)$$

3.3. Effect of Li content on electrical stability

Fig. 2 shows the electrical aging behaviour of NiO films with various Li concentrations. The aging tests were conducted in humid Ar atmosphere at 20% RH. As shown in Fig. 2, the electrical aging rate decreases as the Li concentration increases. According to a previous study,[10] this aging can be attributed to the adsorption of moisture on the NiO surface. The adsorbed water molecules inject electrons into the p-type NiO film, which combine with electrical holes in the film following the reaction: $Ni^{3+} + e^- \rightarrow Ni^{2+}$. This reaction in turn lowers the positive carrier concentration and the electrical conductivity of the film. The adsorption reaction is sensitive to the surface structure of the film and can be suppressed by heating the substrate.[11] In this

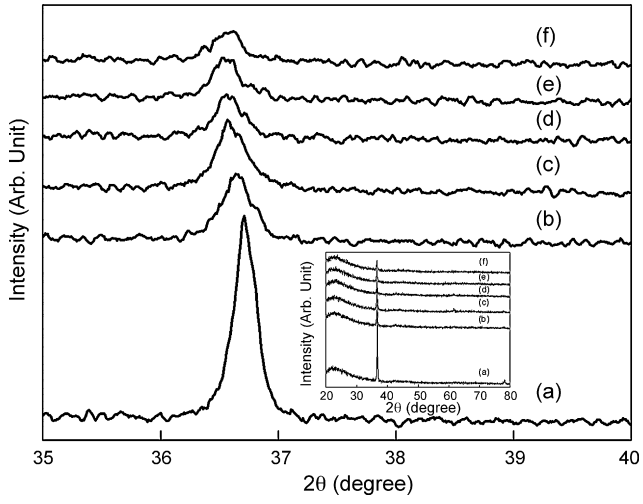

Fig. 3. XRD spectra of NiO thin films with various Li concentrations. (a) un-doped, (b) 0.87 at.% Li, (c) 2.16 at.% Li, (d) 5.49 at.% Li, (e) 11.36 at.% Li, and (f) 16.29 at.% Li. The inset shows the same XRD spectra with a broader two theta range.

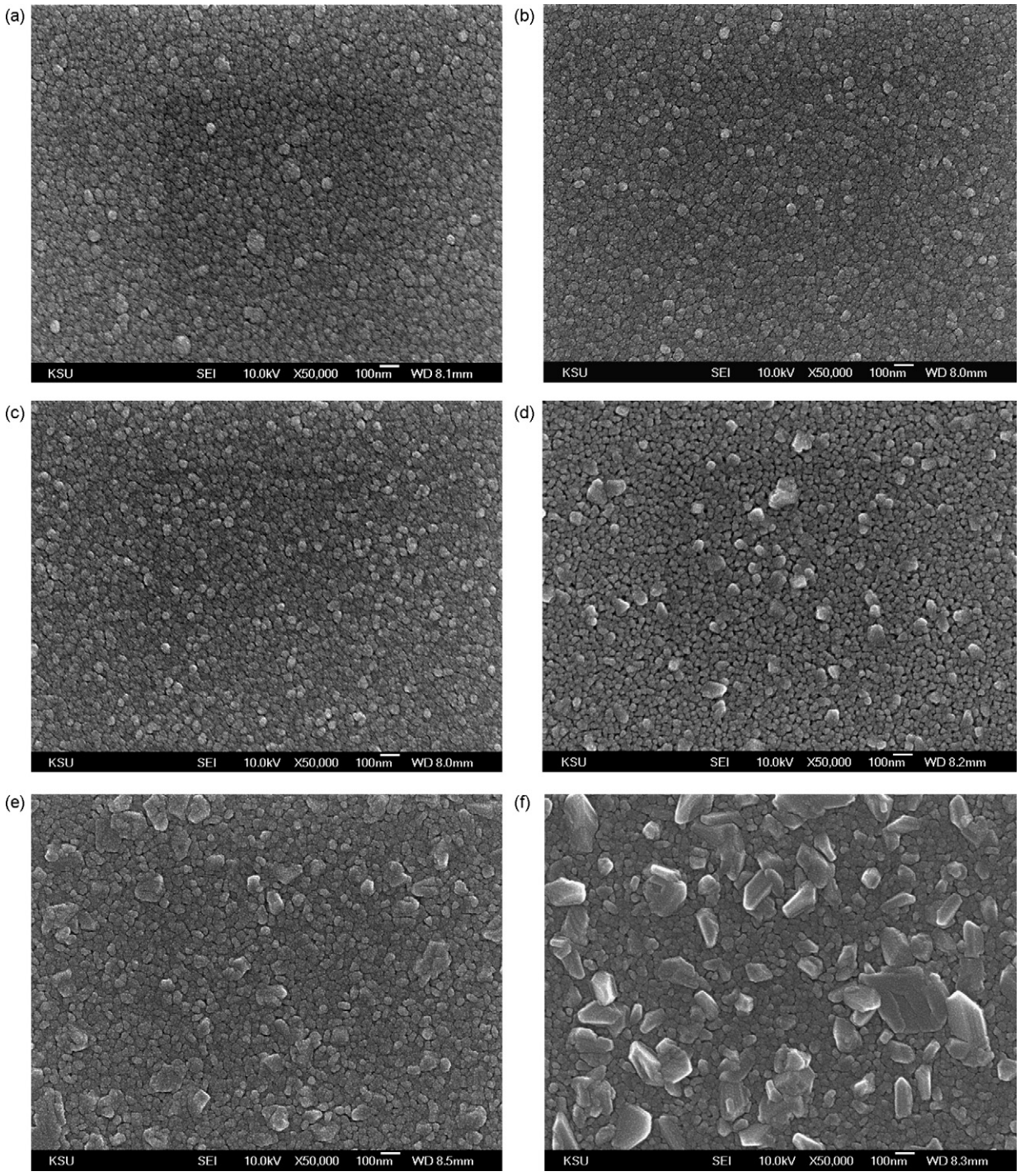

Fig. 4. SEM images of NiO thin films with various lithium concentrations. (a) Un-doped, (b) 0.87 at.% Li, (c) 2.16 at.% Li, (d) 5.49 at.% Li, (e) 11.36 at.% Li, and (f) 16.29 at.% Li.

study, the aging rate of Li-doped NiO film was as low as that for un-doped NiO film prepared when the substrate was heated. In order to understand the effect of Li content on electrical stability, microstructural analyses, including crystallization, surface morphology, material inhomogeneity on the film surface, and the composition profile, were conducted.

Fig. 3 shows the XRD spectra of the NiO films with various Li concentrations. As shown in the figure, there is a (1 1 1) peak in the two theta range. An increase of Li in the NiO films widened the (1 1 1) peak. This suggests that the doping process of the investigated system brought about a progressive decrease in the degree of crystallinity of NiO phases and led to a progressive decrease in their grain size. The (1 1 1) peak shifted towards a low angle as the Li content increased, which means that the doping process increased the lattice constant of the NiO crystal.

For a bulk Ni–Li–O system, Dereń et al. suggested that there is a transition stage in which the first portions of Li occupy the interstitial sites and increase the lattice constant.[5] However,

the critical Li concentration of the transition stage was found to be ~0.2 at.%, which is much lower than our finding. Also, the defect concentration in sputtered NiO is much higher than that in oxidized Ni. The Li ions may more easily fill vacancy sites than interstitial sites. The lattice expansion in this study may be related to the vacancy sites occupied by Li ions. The $Li_xNi_{1-x}O$ solid solutions form over a Li concentration range of $0 \leqq x \leqq 0.5$.[14–16] The crystal structure of these solid solutions changes with x. Two crystal structures of these solid solutions were found in different ranges of x. For $x < 0.3$, lithium cations substitute randomly for nickel cations in the NiO lattice (NaCl-type structure). For $x > 0.3$, ordering of the Li and Ni ions starts in alternating cubic (1 1 1) planes culminating at $x = 0.5$ in layered $LiNiO_2$ (α-$NaFeO_2$ structure). The ordered solid solution is also characterized as $Li_{1-y}Ni_{1+y}O_2$ or $Li_{2x}Ni_{2-2x}O_2$. Chiu[14] reported a shift of XRD peak towards low angle as the crystallographic structure changed from $Li_xNi_{1-x}O$ to $Li_{1-y}Ni_{1+y}O_2$. In this study, the x value ranges from 0 to 0.33. It implies that the shifts in XRD may also be caused by the change in structural symmetry. Therefore, the shifts in XRD peak observed in this study may have been resulted from the combined effect of vacancy sites occupied by Li ions and a change of structural symmetry as Li content increases.

Fig. 4 shows the SEM images of the sputtered films. The surfaces of the sputtered films for Li content below 2.16 at.% are almost the same. The surfaces are smooth and compact. However, some bulges formed on films for Li concentrations above 5.49 at.%. The coverage areas of the bulges increased with increasing Li content, creating more surface area for moisture contact. Semi-quantitative analyses of the bulges were conducted using an Auger electron nanoscope. Fig. 5 shows the Auger spectra of sample (e) on the bulge area and flat surface. The results show that the bulges contain a higher Li concentration than that of the flat surface, which implies that the bulges were formed by segregated Li. A 100 nm thick film prepared under the same conditions as those of sample (e) was investigated by SIMS, as shown in Fig. 6. The SIMS depth profile shows a sharp rise in Li concentration near the surface. Comparing the Auger and SIMS data, it can be found that doped Li segregated near the surface to yield bulges on the film. A similar Li–O layer on the film surface of sputtered lithium nickel oxide was found by Chiu.[14] The Li–O layer possibly formed due to the large negative standard heat of formation of the lithium-based oxides. Li elements that segregated on the grain boundary were also found in Li-doped ZnO films with increased Li content.[17] These results imply that doped Li ions prefer to aggregate in crystal defect sites such as vacancies, grain boundaries, and surfaces, possibly decreasing the crystal distortion and total free energy of the film.

The above results indicate that the surface morphology, crystallization, and composition uniformity changes are all related to Li doping. The effects of surface morphology and crystallization on suppressing the aging rate are relatively small and may be neglected due to the increase of surface area and the decrease of grain size, which always enhance for reaction rate. The decrease in aging rate with increasing Li concentration may be due to the Li-rich oxides segregated near the film surface. As mentioned above, the electrical aging behaviour results from the reaction between moisture and the holes in Ni^{3+}. The Li-rich oxide on the film surface could serve as a dense protective barrier layer between NiO film and water moisture. This decreases electrical aging and leads to a relatively stable conductivity.

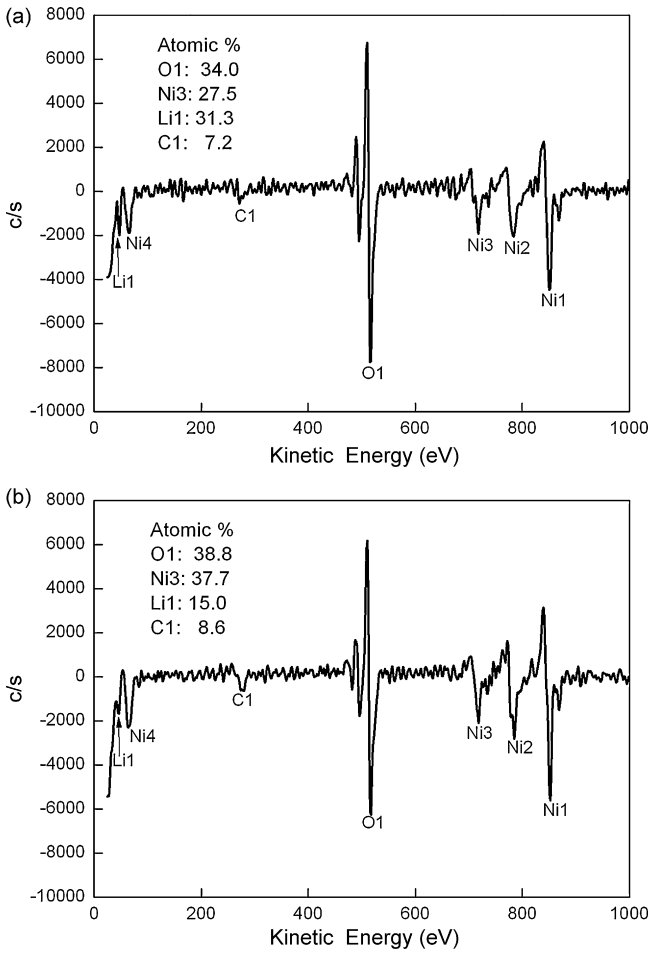

Fig. 5. Auger spectra of Li-doped NiO film (a) in bulge area and (b) in flat plane.

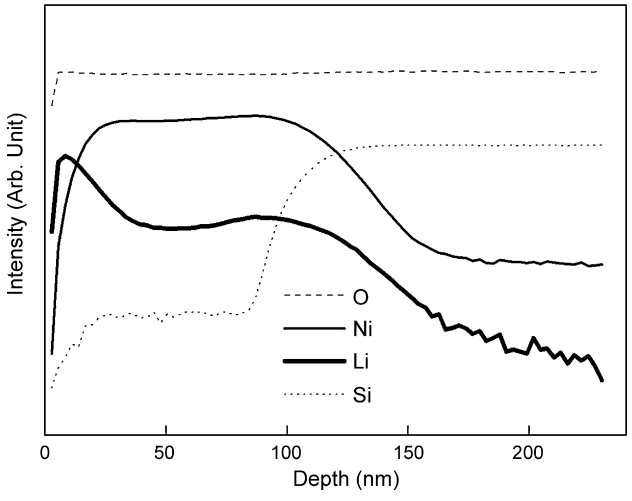

Fig. 6. SIMS depth profile of Li-doped NiO film.

4. Conclusions

Pure NiO and Li-doped NiO films were deposited on Corning 1737 substrates by RF reactive magnetron sputtering using Li_2O pieces as the doping source. Film composition, resistivity, electrical stability, and microstructure were examined. The results can be summarized as follows.

Increasing the number of Li_2O disks was found to effectively increase the Li content in the NiO films. The O/Ni ratio and the electrical conductivity slightly decreased with a small amount of Li in the NiO films because the first portions of Li filled the nickel vacancies. With increasing Li dopant concentration, some Li-rich oxides segregated near the film surface and formed bulges. Li doping did not significantly decrease the electrical resistivity, but it effectively suppressed electrical aging by forming a dense Li-rich oxide near the film surface. Thus, the electrical stability of NiO films can be improved by Li doping.

Acknowledgments

The authors would like to thank the National Science Council of Taiwan for financially supporting this research under grants NSC 95-2221-E-006-081-MY3, NSC 96-2622-E-024-003-CC3, and NSC 96-2221-E-024-020-MY3.

References

1. Sato, H., Minami, T., Takata, S. and Yamada, T., Transparent conducting p-type NiO thin films prepared by magnetron sputtering. *Thin Solid Films*, 1993, **236**, 27–31.
2. Chan, I. M. and Hong, F. C., Improved performance of the single-layer and double-layer organic light emitting diodes by nickel oxide coated indium tin oxide anode. *Thin Solid Films*, 2004, **450**, 304–311.
3. Korošec, R. C. and Bukovec, P., Sol–gel prepared NiO thin films for electrochromic applications. *Acta Chimica Slovenica*, 2006, **53**, 136–147.
4. Hotovy, I., Huran, J., Siciliano, P., Capone, S., Spiess, L. and Rehacek, V., Enhancement of H_2 sensing properties of NiO-based thin films with a Pt surface modification. *Sensors and Actuators B*, 2004, **103**, 300–311.
5. Jarzebski, Z. M., Oxide Semiconductors, Pergamon Press, Oxford, 1973, pp.150, 184–186.
6. Kang, J. K. and Rhee, S. W., Chemical vapor deposition of nickel oxide films from $Ni(C_5H_5)_2/O_2$. *Thin Solid Films*, 2001, **391**, 57–61.
7. Reguig, B. A., Khelil, A., Cattin, L., Morsli, M. and Bernède, J. C., Properties of NiO thin films deposited by intermittent spray pyrolysis process. *Applied Surface Science*, 2007, **253**, 4330–4334.
8. Puspharajah, P., Radhakrishna, S. and Arof, A. K., Transparent conducting lithium-doped nickel oxide thin films by the spray pyrolysis technique. *Journal of Materials Science*, 1997, **32**, 3001–3006.
9. Joshi, U. S., Matsumoto, Y., Itaka, K., Sumiya, M. and Koinuma, H., Combinatorial synthesis of Li-doped NiO thin films and their transparent conducting properties. *Applied Surface Science*, 2006, **252**, 2524–2528.
10. Jang, W. L., Hwang, W. S. and Lu, Y. M., Effect of different atmospheres on the electrical stabilization of NiO films. *Vacuum*, 2009, **83**, 596–598.
11. Jang, W. L., Hwang, W. S., Lu, Y. M., Hsiung, T. L. and Wang, H. P., Effect of substrate temperature on the electrically conductive stability of sputtered NiO films. *Surface & Coatings Technology*, 2008, **202**, 5444–5447.
12. Kofstad, P., *High Temperature Corrosion*. Elsevier Applied Science, London and New York, 1988, pp. 100–101.
13. Kofstad, P., *Nonstoichiometry, Diffusion, and Electrical Conductivity in Binary Metal Oxides*. John Wiley and Sons, New York, 1972, pp. 246–251.
14. Chiu, K. F., In situ modification of RF sputter-deposited lithium nickel oxide thin films by plasma irradiation. *Journal of The Electrochemical Society*, 2004, **151**(11), A1865–A1869.
15. Abraham, D. P., Twesten, R. D., Balasubramanian, M., Kropf, J., Fischer, D., McBreen, J., Petrov, I. and Amine, K., Microscopy and spectroscopy of lithium nickel oxide-based particles used in high power lithium-ion cells. *Journal of The Electrochemical Society*, 2003, **150**(11), A1450–A1456.
16. Azzoni, C. B., Paleari, A., Massarotti, V., Bini, M. and Capsoni, D., Cationic and magnetic order in $LiNiO_2$- and NiO-type Li–Ni mixed oxides. *Physical Review B*, 1996, **53**(2), 703–709.
17. Fujihara, S., Sasaki, C. and Kimura, T., Effects of Li and Mg doping on microstructure and properties of sol–gel ZnO thin films. *Journal of the European Ceramic Society*, 2001, **21**, 2109–2112.